



## Fluorescent N-doped Carbon Dot-Copper and Silver Nanocomposite - An effective uric acid sensor

Dona Mary Sam & Mary Vergheese T\*

Department of Chemistry, Madras Christian College, Tambaram East, Chennai-600 059, Tamil Nadu, India

Received 15 December 2020; revised 05 April 2021

Green fluorescent Nitrogen doped Carbon Dots (N-CDs) was synthesized by solvent free pyrolysis technique. Using the synthesized N-CDs, for first time we report the synthesis of Blue fluorescent Nitrogen doped silver and copper carbon dot nano composite using a Simple, Solvent free Green method. The N-CDs function as reducing agent to reduce  $\text{Ag}^+$  and  $\text{Cu}^{2+}$  ions to  $\text{Ag}^0$  and  $\text{Cu}^0$  which leads to the formation of composite. The synthesized N-CDs and nano composites were applied as Uric Acid(UA) sensor. N-CDs and the composites function as a fluorophore in the recognition of Uric acid. Both the N-CDs and the composites were characterized using UV-Vis, FTIR, SEM-EDX, TEM and PL spectroscopic techniques. The UV-Vis and FTIR response of N-CDs in comparison with N-doped silver and N-doped copper carbon dot composites confirms that the surface functional groups on N-CDs have been used in the formation of silver and copper carbon dot composite. The surface morphology and elemental composition of synthesized carbon dots and its nanocomposites were identified using SEM-EDAX analysis. High resolution transmission electron microscopy (HR-TEM) analysis shows that N-Cdot are spherical in shape with an average size of 15.23 nm, Cu/N-Cdot composite is found to be spherical and the size to be in the range of 18.02 nm and Ag/N-Cdot composite is found to be spherical and the size of the composite is found to be 16.40 nm. The PL spectra was also observed for Cu/N-Cdots, Ag/N-Cdots. With addition of Uric acid there was a quench in fluorescence which is immediately visible by our naked eye. The quench in fluorescence is due to the synergistic effect between the fluorescence Inner Filter Effect (IFE) and the static quenching effect, with a Lower detection limit (LDL) of  $4\mu\text{M}$  thus functioning as a highly rapid UA biosensor. Simple naked eye observation and the absence of catalytic effect by the metal ion in the detection of UA are the merits of the present study.

**Keywords:** Copper/N-doped carbon dot, N-doped carbon dots, Silver/N-doped carbon dots, Uric acid sensor

Heteroatom doped Carbon dots provide effective binding site and incorporates surface modifications such that they function as effective Fluorescent sensors. The ratio of the hetero atom to the carbon content can be varied depending on the type of synthesis which also alters the optical property of Doped CDs. Compared to Non doped CDs, the doped CDs function as effective sensors since their excitation wavelength shifts from 260-320 nm to higher wavelength and the emission band may shift to green, yellow and red. If the functional groups of the heteroatom doped CDs do not function as an effective sensor, they can be modified by the addition of biopolymers, organic moieties through substitution, elimination, condensation, dehydration, carbonization reactions to obtain specific sites for binding<sup>1</sup>. The fluorescence nature of NCDs is tuned based on the surface groups and also by using various precursors for synthesis<sup>2-4</sup>. Because of the attractive properties

of N-CDs like photo stability, ease of solubility in aqueous medium, tunable photoluminescence, biocompatibility they are used as suitable candidates in the field of sensors, bioimaging, catalysis etc<sup>5</sup>. The recognition of biomolecules has become a vital need in the field of medicine, food, environment etc. Uric Acid (UA) being a major catabolite of purine metabolism in the human system<sup>6</sup> has a pKa of 5.75. Since it is present in body fluids like serum and urine it functions as an important biomarker in clinical diagnosis for diseases such as gout, hyperuricemia or Lesch-Nyan Syndrome<sup>7</sup>. The normal level of uric acid in serum is between 0.13 and 0.46 mM (2.18-7.7 mg dL<sup>-1</sup>)<sup>8</sup> and 1.49-4.46 mM (25-74 mg/dL) in urine<sup>9</sup>. Abnormal levels of UA in body fluids leads to cardiovascular, neurological, hypertension, and renal insufficiency related diseases. As a result, its determination and diagnosis are a prerequisite for physiological investigations. Recognition of UA is carried out using various analytical techniques like Chromatography<sup>10</sup>, electrochemistry<sup>11,12</sup> and spectroscopic methods<sup>13-15</sup>. NCDs due to their

\*Correspondence:  
E-mail: maryvergheese@mcc.edu.in

multicolour photoluminescence(PL) makes them a suitable candidate in the field of sensors. Recently doped CDs with metal and noble metals are used as fluorometric sensors<sup>16-18</sup> have been used in the recognition of biomolecules, here we report the synthesis of N-CDs and their silver and copper composite. The composites were synthesized using solvent free pyrolysis method, characterized using UV-Vis, SEM-EDX, HR-TEM and PL spectroscopy. The synthesized N-CDs and its composites function as a fluorophore and based on the Inner Filter Effect and quenching phenomenon they successfully function as an UA sensor.

### Materials and Methods

All the chemicals used in the study were of extra pure analar grade and hence without further purification they were used for the analysis. Ethanolamine was purchased from Sisco Research Laboratories, Hydrogen peroxide (H<sub>2</sub>O<sub>2</sub>) 6% solution from PS Laboratories, Uric acid from Scientific Chemicals, KH<sub>2</sub>PO<sub>4</sub> from Nice Chemicals, Na<sub>2</sub>HPO<sub>4</sub> from Nice Chemicals, Cupric sulphate from Chemspure, Silver Nitrate from Spectrum Chemicals and Reagents. All solutions were prepared using Distilled water. Phosphate buffer of pH 6.8 was used for the sensor studies towards recognition of UA.

#### Synthesis of N-CDs, Copper /N-Carbon dot nanocomposite (Cu/N-CDs) and Silver /N-Carbon dot nanocomposite (Ag/N-CDs)

N-CDs were synthesized as reported in earlier literature<sup>19,20</sup>. For the synthesis of Cu/N-CDs, in a clean dry beaker 3 mL of ethanolamine was taken and 4.5 mL hydrogen peroxide was added, to that 10 mL of 5 mM copper sulphate solution was added and heated at 150°C for 7 min. The solution was completely vaporized and a black residue was obtained which is copper/N-Carbon dot nanocomposite, the residue shows blue fluorescence under UV radiation confirming the formation of Cu/N-C-dots<sup>21</sup>. It was also confirmed with SEM-EDX analysis. The residue is used for further studies. For the synthesis of Ag/N-CDs in a clean beaker 3 mL of ethanolamine is added to 4.5 mL hydrogen peroxide, to that 10 mL of 5mM silver nitrate solution was added and heated at 150°C for 7 min. The solution was completely vaporized and a black residue was obtained which is Ag/N-CDs. The residue shows blue fluorescence under UV radiation confirming the formation of silver/ N-C-dots<sup>22</sup>. For the sensor studies 0.01 g of N-CD and its composite were used.

### Characterization Studies

UV-Vis studies were conducted using Elico SL20 Double Beam UV-Vis spectrophotometer in the range of 200-800 nm. Surface functionalized Carbon Dots are stable in water through the formation of an extensive hydrogen bonding network<sup>23</sup>. Fourier Transform-Infrared Spectroscopic Analysis was carried out using KBr pellet method in the range 400-4000 cm<sup>-1</sup> using SHIMADZU IR AFFINITY 1. Surface morphological studies and elemental analysis was carried out using FEI Quanta 200 F High Resolution Scanning Electron Microscopy with Energy dispersive X-ray diffractometer. HRTEM analysis of the sample was done using TEM-2100 plus High-Resolution Tunneling Electron Microscopy. Very small amount of N-CDs, was dissolved in ethanol, sonicated for 15 min and 10 micro litre of the sample was taken and dispersed on the copper grid. The copper grid was further dried in hot air oven for 30 min at 60°C and analysis was carried out. The same procedure was carried out for the composites too for HR-TEM analysis. Photoluminescence Analysis (PL) was performed using Jascospectrofluorometer FP-8300.

#### Protocol used for the Detection of UA using N-CDs, Cu/N-CDs and Ag/N-CDs

To 0.01g of N-CDs, 10 mL of phosphate buffer was added and stirred for 15 min to get a homogeneous solution. The pH of the solution was maintained at 6.8. Further, to this solution 1 mL additions of 1 mM of uric acid (UA) was added and stirred for a few min. With every 1 mL addition, the change in absorbance was measured using UV-Vis, change in fluorescence was measured using PL techniques. The same procedure was repeated for different concentrations of UA *i.e.*, 1 Milli molar, 10 Milli molar, and 100 Milli Molar. Similarly for the detection of UA using Cu/N-CDs and Ag/N-CDs 0.01 g of each was taken separately and the above procedure was repeated.

### Results and Discussion

#### Synthesis of N-CDs

During the synthesis of N doped Cdots, color change was observed. *i.e.*, from bright yellow to orange red which indicates the polymerization step is in progress and finally a dark colored solution is obtained which confirms that the carbonization process is complete<sup>23</sup>. On complete vaporization of the residue N-Cdots was obtained (Fig. 1A). It was collected, stored at room temperature and used for

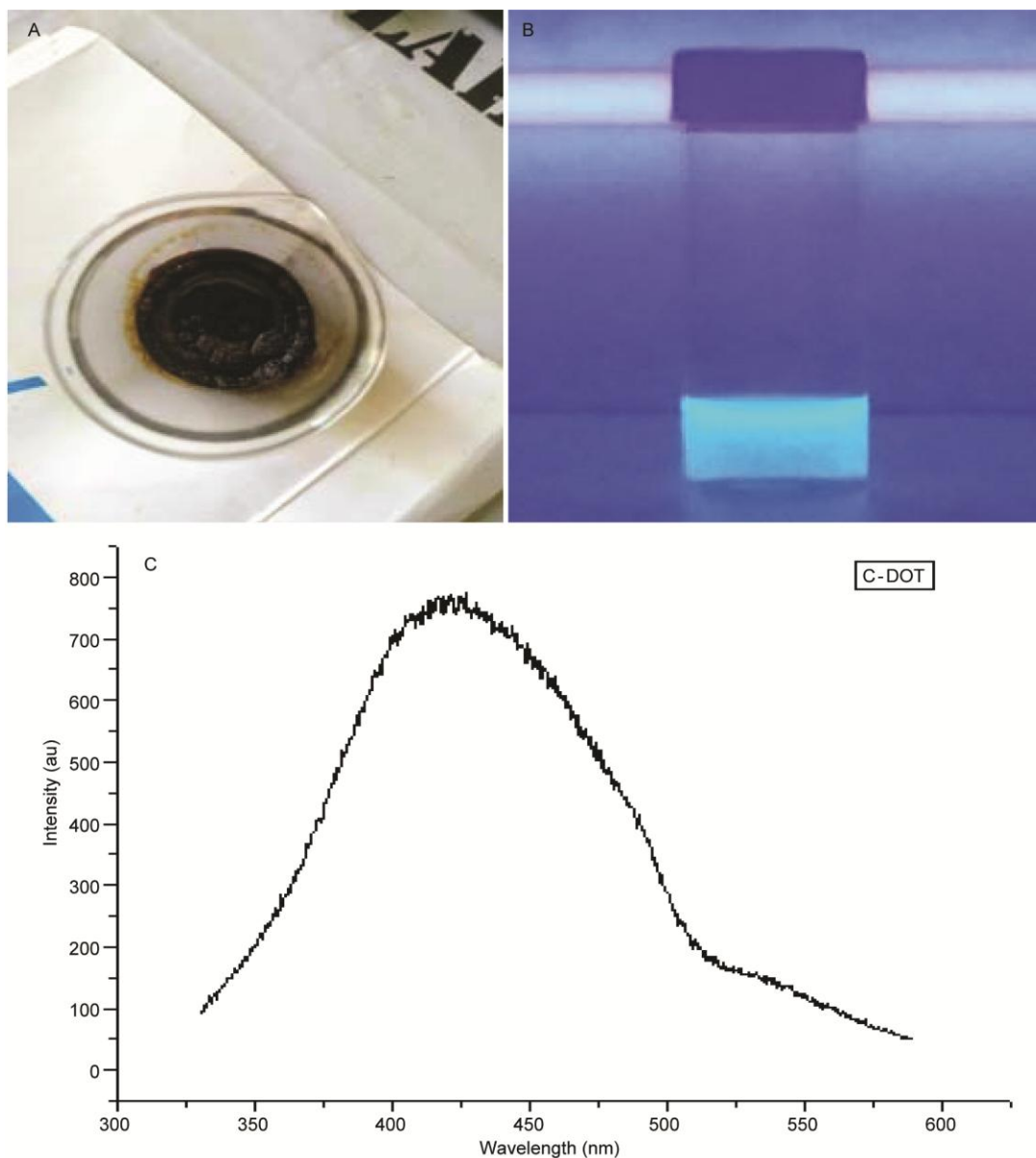


Fig. 1 — (A) synthesized N-CDs; (B) N-Cdot under UV light; and (C) PL response of N-Cdot

characterization and application studies. The N-CDs obtained was found to be highly soluble in aqueous solution conforming a high content of surface polar organic groups containing carbon, nitrogen and oxygen<sup>24</sup>. A bright GREEN fluorescence was observed (Fig. 1B) for N-CDs which is due to the increased amount of surface passivation caused due to hydrogen peroxide which is in accordance to earlier reports<sup>23</sup>. The green emission (longer wavelength) is due to the intrinsic state emission (electron-hole recombination)<sup>25</sup>. The photoluminescence spectra of N-CDs shows peak intensity at 750 au at  $\text{cm}^{-1}$  (Fig. 1C). This behavior is attributed to the surface

state affecting the band gap of the carbon dots<sup>26</sup> *i.e.* the fluorescence originate from the transition of lowest unoccupied molecular orbital (LUMO) to the highest occupied molecular orbital (HOMO). The HOMO-LUMO gap depends on the size of the N-CDs and stronger luminescence is observed in smaller C-dots. The polygonal structure of N-CDs from the SEM-EDAX value also confirms arm chair edge and hence reason for increased luminescence<sup>27</sup>. The N-CDs were found to be stable in solution at room temperature for more than 2 months and also exhibited fluorescence. This stability is due to the amorphous nature of N-CDs<sup>28</sup>.

### Synthesis of Copper/C- dot composite

Figure 2A shows the synthesis of Cu/N-C-dot. It is observed that in the process of synthesizing the composite the colour changes from blue to yellow and then to reddish orange and finally to black solution, conforming the formation of Cu/N-Cdot composite. From (Fig. 2B) it is observed that there is a blue luminescence is observed compared to N-doped carbon dot *i.e.* absorbance is shifted towards shorter wavelength. The photoluminescence spectra of Cu/N-Cdot show peak intensity occurs at 900 au as shown in (Fig. 2C). A blue shift compared to that of N-CDs. Large number of amine groups and

oxygen rich groups on the surface of carbon dots function as receptors<sup>21</sup> and capture the copper ions through metal coordination to form a complex whose absorption band overlap partially with the emission spectra of carbon dots. The blue fluorescence may be because the Cu<sup>2+</sup> ions may be attached to the carboxyl groups and hydroxyl groups of N-CDs and not to the nitrogen moiety. Thus no quench in fluorescence is observed<sup>29</sup>. Cdots also function as reducing agent as they are excellent electron acceptors and electron donors<sup>30</sup>. The hydroxyl and carboxyl groups on the surface of CQDs play an important role such that N-CDs

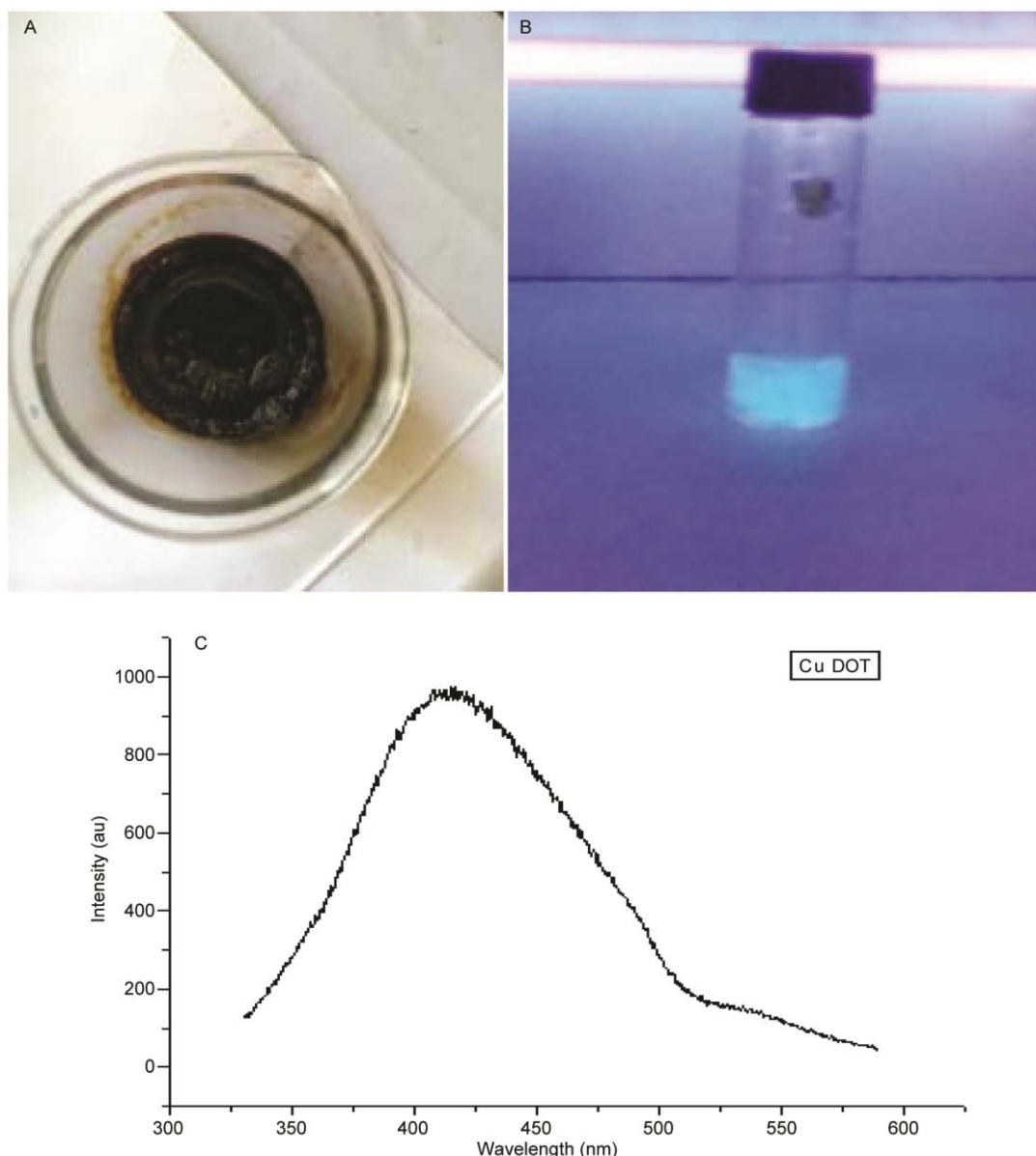


Fig. 2 — (A) Cu/N-CDs; (B) Cu/N-CDs under UV radiation; and (C) PL response of Cu/N-CDs

function as reducing agent and also lead them to be the nucleation centres for the growth of metallic nanoparticles<sup>31</sup>. Herein, N-CDs function as the reducing agent like citrate, ascorbates and sodium borohydride.

#### Synthesis Ag-Carbon dot composite

From Figure 3A shows the synthesis of Ag/C-dot composite. From Figure 3B it is observed that there is a blue luminescence compared to the green luminescence observed in N-doped carbon dot composite solution, which is due to inner filter effect<sup>32</sup>. The photoluminescence spectra of Cu/N-CDot

show peak intensity at 850 au in (Fig. 3C), a shift towards lower wavelength compared to N-CDs. Large number of carboxyl, hydroxyl and oxygen rich groups on the surface of carbon dots function as receptors and capture the silver ions through metal ion coordination forming a complex whose absorption band overlap partially with the emission spectra of carbon dots<sup>33</sup>. This results in the blue fluorescence<sup>34</sup>. The C-dots have the ability to directly reduce of  $\text{Ag}^+$  to  $\text{Ag}^0$  without the addition of any external reducing agent. By just incubating  $\text{Ag}^+$  with C-dot for 5 min, Ag NP's grow on carbon dot. This involves the oxidation of amine or phenolic hydroxyl group on

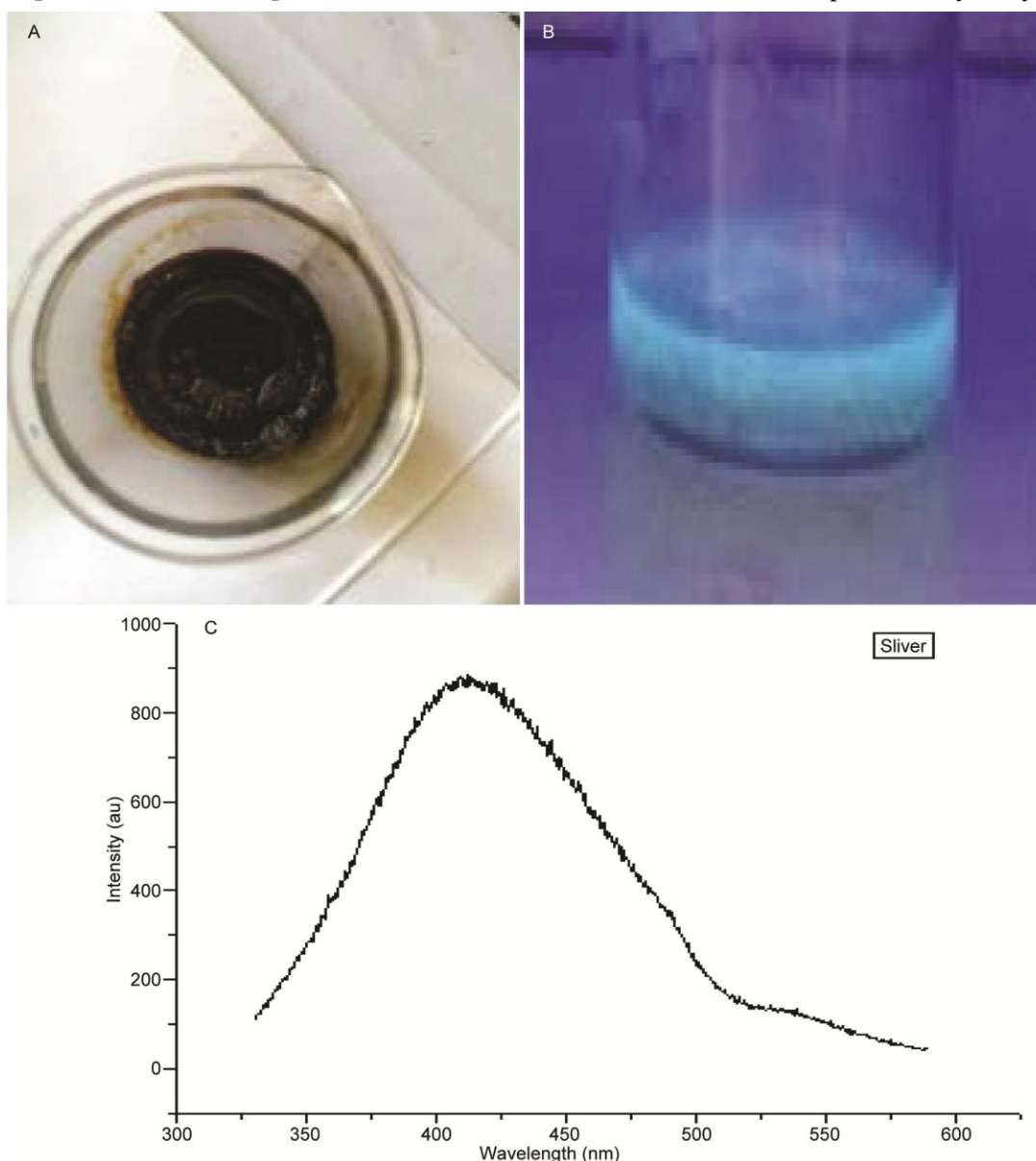


Fig. 3 — (A) Ag/N-CDs; (B) Ag/N-CDs under UV radiation; and (C) PL response of Ag/N-CDs

aromatic ring of C-dot. The C-dot functions as a reducing and stabilizing agent for the formation of Ag/N-Cdot composite.

#### UV-Visible, FTIR, XRD, SEM- EDX, TEM response of the synthesized N-Cdot, Cu/N-Cdot, Ag/N-Cdot

The UV response observed at 350 nm in (Fig. 4A) confirms the formation of N-CDs<sup>35</sup>. Thus N-CDs dots with higher oxidation degree poses bright luminescence, the high fluorescence emission of N-CDs is attributed to the radiative recombination of their surface-confined electrons and holes<sup>29</sup>. Figure 4B & C shows UV-Vis absorption spectrum for Cu/N-C-dot composite and Ag/N-C-dot composites with a shoulder at 282 nm and 268 nm. On comparing the UV response of the composite with N-CDs, it is observed that the absorbance peak is shifted to lower wavelength which confirms the formation of composite, this is further confirmed with the change in fluorescence from green to blue. As N-CDs reduce the  $\text{Cu}^{2+}$  and  $\text{Ag}^+$  salt, nucleation gets initiated at the surface sites which host the electrons, thus the electron-hole recombination process on N-CDs surface is disrupted, leading to blue fluorescence *i.e.* a shift towards shorter wavelength<sup>30</sup>.

On comparing Figure 5B with 5C it is observed that the intensity of the peak in the N-CD composite is reduced compared to pure N-CDs. The peak between  $3000\text{--}3500\text{cm}^{-1}$  which is due to the  $\text{--OH}$  stretching is reduced and found to be broad in (Fig. 5B) on comparing with pure N-CDs. Weak peaks ranging from  $2500\text{--}3000\text{cm}^{-1}$  are due to C-H stretching vibration of  $\text{CH}_2$  and  $\text{CH}_3$  groups. The strong peak at  $1400\text{cm}^{-1}$  in (Fig. 5B) corresponds to C-N stretching. The peak at  $1360\text{cm}^{-1}$  confirms the symmetric stretch of N-O due to the oxidized amido group. The peak at  $1600\text{cm}^{-1}$  shows the C=O stretching of the amide bond. The peak at  $1271\text{cm}^{-1}$  is the stretching vibration of the benzene ring linked to tertiary amine or aryl ether  $=\text{C-O-C}$ . The peak at  $1060\text{cm}^{-1}$  confirms the symmetrical stretching vibration peak of aryl ether. The peak at  $782\text{cm}^{-1}$  corresponds to C-H stretch. On comparing the FTIR response between N-Carbon dot, silver/N-Cdot and copper/N- carbon dot composites it is clear that the in plane and out of plane bending vibrations of OH at  $1300\text{--}1500$  and at  $650\text{cm}^{-1}$  and the intensity of C=O vibrational absorption at  $1670\text{cm}^{-1}$  is decreased. This confirms that the surface functional groups on N-carbon dots have been used in the formation of silver and copper carbon dot composite.

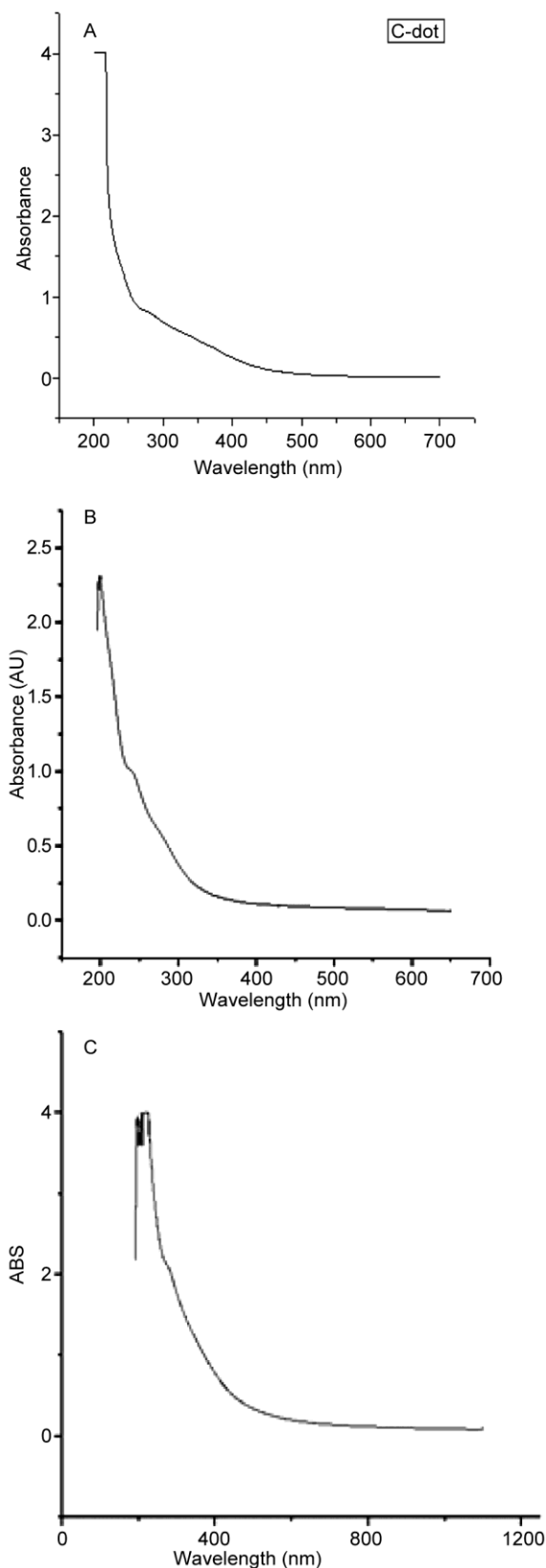


Fig. 4 — (A) UV-Vis spectrum of N-doped CDs; (B) UV-Vis spectrum of Cu/N-CDs; and (C) UV-Vis spectrum of Ag/N-CDs

Figure 6A shows the SEM image of N-doped Carbon dots. The C-dots are found to be polygonal in shape *i.e.* arm chair edge. The dimensions of C-dot were found to be in the range between 22 and 72 nm which is also confirmed from XRD studies. The EDAX response, (Fig. 6B & C) depicts the elemental composition of N-doped Carbon dot. The weight percentage of carbon was found to be 62.32

Figure 6D shows the SEM image of Cu/ N-Cdot composite. It is found that the composite are spherical in shape. Its dimensions were found to be in the range of 84 and 105 nm. Figure 6D & E represents the elemental composition of Cu and N-CDs using EDX. The weight percentage of carbon and copper was found to be 58.98 and 3.14

SEM image of Ag/C-dot composite (Fig. 6G) illustrates its dimensions to be in the range between 62 and 142nm. Figure 6H & I depicts the elemental composition of Ag/C-dot Nano composite using EDAX. The weight percentage of silver and carbon was found to be 13.77 and 51.53.

From the HR-TEM image of N-CDs (Fig. 7A) it is observed that the particles are spherical in shape and fitting the histogram to a Gaussian model with mean diameter of  $15.23 \pm 2$  nm. Figure 7B shows the HR-TEM image of Cu/N-Cdot Composite. They are also found to be spherical and fitting the histogram to a Gaussian model the mean diameter is 18.2 nm. Figure 7C shows the Ag/N-Cdot Composite which are found to be spherical and fitting the histogram to a gaussian model the mean diameter of the composite is found to be 16.40 nm.

#### Detection of Uric acid using N-Cdots, Cu/N-Cdot nanocomposite, Ag/N-Cdot nanocomposite

Figure 8A shows the quench in fluorescence with addition of 1mM uric acid, It is also confirmed by the decrease in absorbance observed from Fig. 8(B & C)

UV-VIS spectra and photo colorimeter response *i.e.* The quench in fluorescence observed with addition of UA when compared to N-CD is because of the synergistic effect between the fluorescence Inner Filter Effect (IFE) and the static quenching effect. With every addition of UA the absorbance decreases and similarly a quench in fluorescence is also observed. Thus N-C dot is able to function as a fluorophore to sense UA. The quench in fluorescence is observed immediately with the addition of UA. The decrease in fluorescence is observed easily by the naked eye.

Figure 9A shows decrease in intensity of blue fluorescence with every 1 mL addition of 1mM uric acid *i.e.*, fluorescence is found to be quenched, which is also confirmed by the decrease in absorbance measured using UV-Vis spectra results which support the above findings (Fig. 9B & C). Thus, similar to N-C dot the quench in fluorescence is because of the synergistic effect between the fluorescence internal filtering effect and the static quenching effect. At the surface sites that host the electrons, the electron-hole recombination process were disrupted which led to fluorescence quenching effect. The quench in absorbance is observed immediately with addition of UA to the composite solution.

#### Detection of Uric acid using Ag/N-Cdot nanocomposite

Figure 10A shows a blue fluorescence of Ag/N-C dot observed in presence of UV radiation in presence of 1 mM UA. The hydroxyl and carboxyl groups in the surface of N-Cdot serve as reducing and stabilizing centres for the reduction of  $\text{Ag}^+$  to  $\text{Ag}^{0}$ . On comparing the fluorescence with Ag/N-Cdot, it is observed that with every 1 mL addition of 1 mM uric acid, there is a quench in fluorescence, which is also confirmed by the decrease in absorbance measured

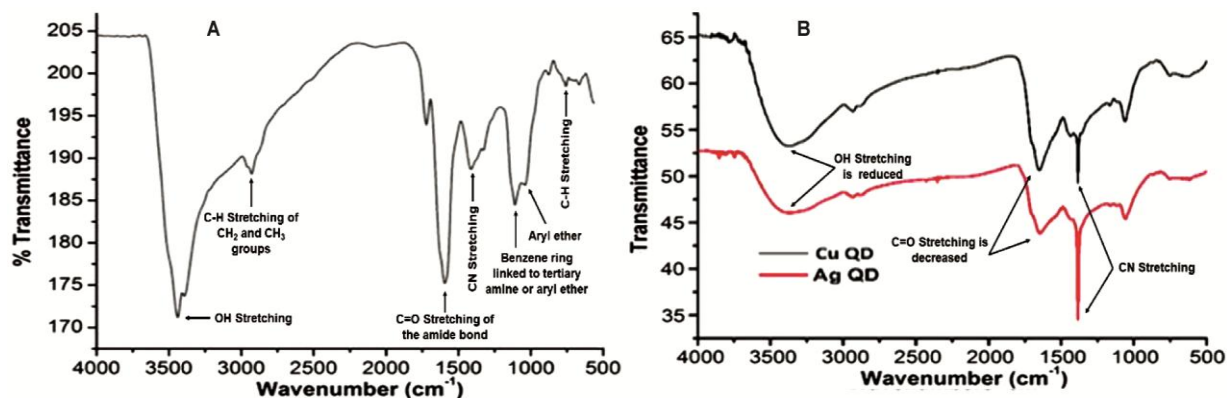


Fig. 5 — FTIR spectrum of (A) N-C dots; and (B) Ag/N-CDs and Cu/N-CDs

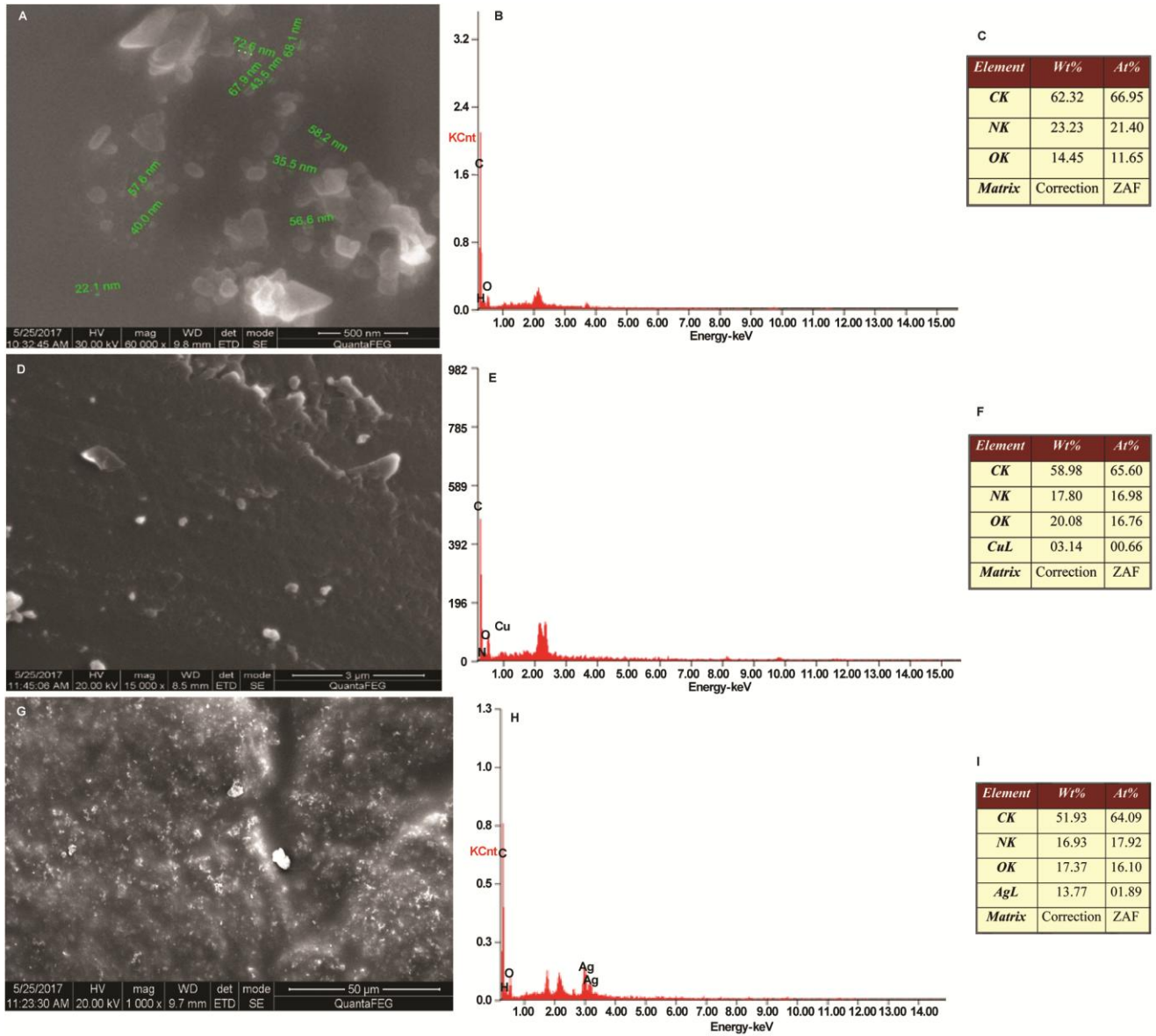


Fig. 6 — (A) SEM Image of N-CDs (B & C) EDAX response of N-CDs; (D) SEM image of Copper/N-CDs (E & F) EDX response of Copper/N-CDs; (G) shows the SEM image of Ag/N-CDs; and (H & I) EDX image of Ag/N-CDs

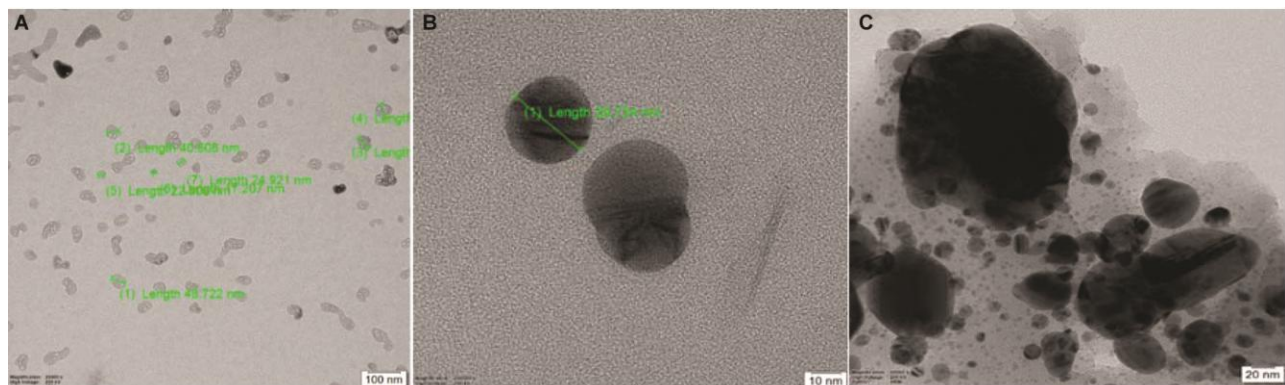


Fig. 7 — High-Resolution Transmission Electron Microscopy image of (A) N-CDs; (B) Cu/N-CDs; and (C) Ag/N-CDs



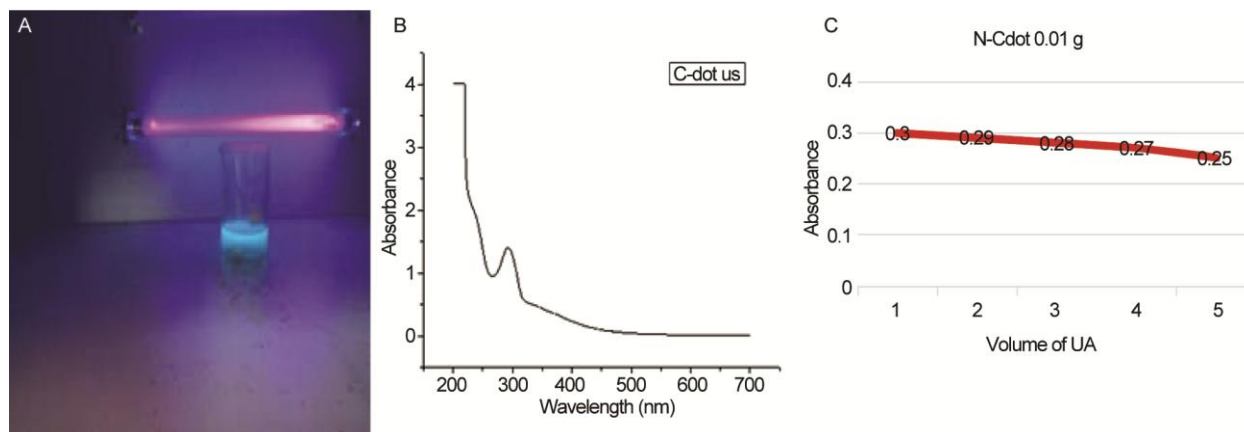


Fig. 8 — (A) N-C-dot +UA (1 mM); (B) UV-Vis response for N-Cdot with 1 mM UA addition; and (C) Change in Absorbance with 1 mL additions of UA

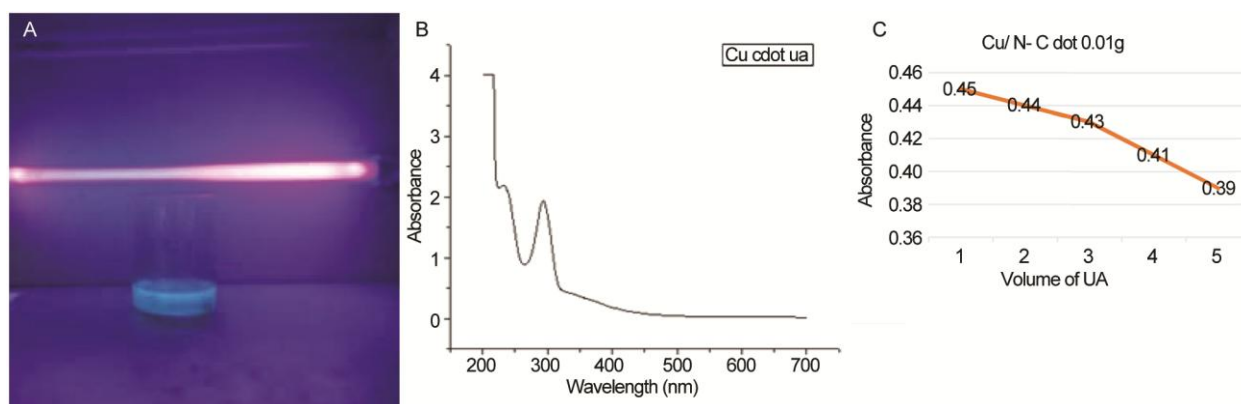


Fig. 9 — (A) Cu/N-Cdot +UA (1 mM); (B) UV-Vis response of Cu/ N-Cdot+ UA (1mM); and (C) Change in Absorbance with additions of 1 mM UA

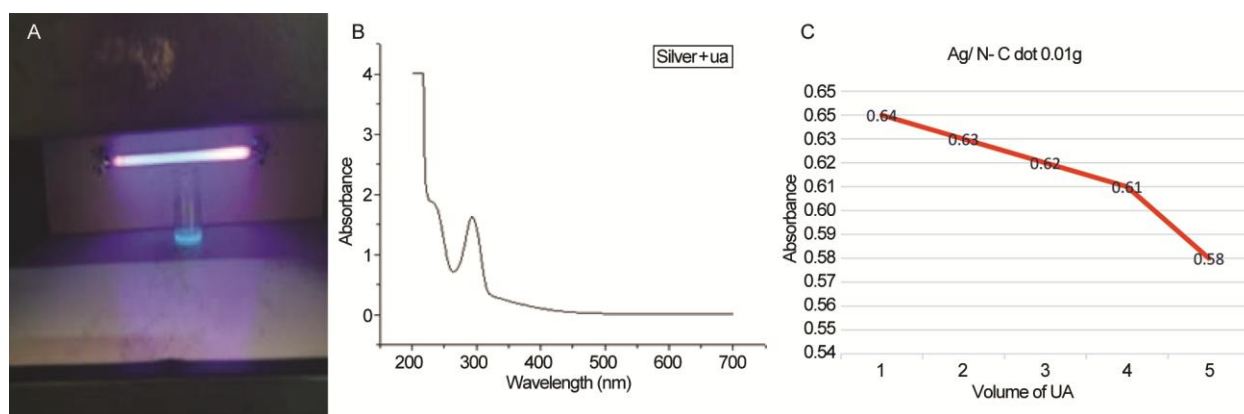


Fig. 10 — (A) Ag/N-Cdot +UA (1 mM); (B) UV-Vis response of Ag/N-Cdot+ UA (1 mM); and (C) Change in absorbance with additions of 1 mM UA

using UV-Vis spectra results (Fig. 10B & C). The surface sites that host the electrons, the electron-hole combination processes on N-CDs were disrupted because of the electrostatic and hydrogen bonding<sup>37-40</sup> formed between the UA and N-Cdots, leading to fluorescence

quenching effect. The quench in absorbance is observed immediately with addition of UA to the composite and similarly in all the cases it is observed that the quench in fluorescence was found to have a linear decrease in absorbance with increase in addition of UA.

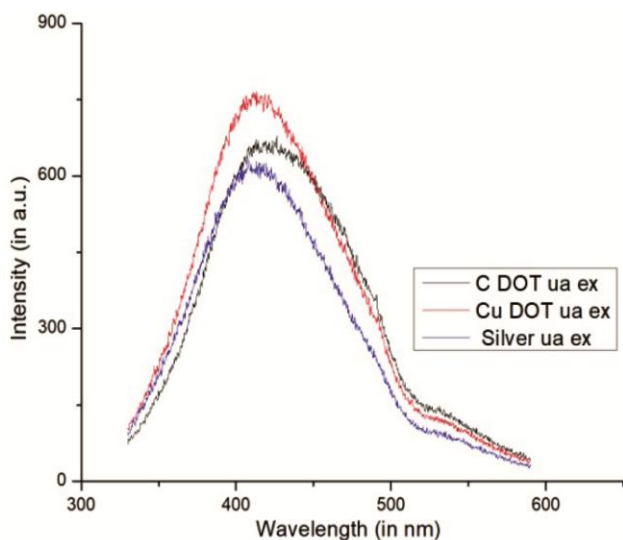


Fig. 11 — Detection of UA by N-CDs, Cu/N-CDs, Ag/N-CDs

#### Comparison of N-C dot, Cu/ N-Cdot and Ag/N-Cdot as an effective UA biosensor

The PL response in Figure 11 compares all the three systems towards sensing of UA. It is observed that all the three systems exhibit quench in fluorescence on addition of UA, the quench in fluorescence is considered as an analytical signal towards recognition of UA. No catalytic effect is observed on UA due to the presence of metal ions. The pKa of uric acid is 5.75 and it is a weak acid. As a result of this uric acid gets easily ionized and bonds with the surface groups present on N-Cdots, Cu/N-Cdots and Ag/N-C dot leading to quenching in fluorescence. The interaction of molecules or ions with the surface groups of the C-dots can affect the recombination of electron hole<sup>41-44</sup>. A lowest detection limit towards sensing of UA is found to be 4  $\mu\text{M}$ . The response by the system is also rapid. Thus N-Cdot, Cu/N-Cdot, and Ag/N-Cdot function as an effective and rapid UA biosensor.

#### Conclusion

In this work N-CDs, Cu/N-CDs and Ag/N-CDs were synthesised using the precursor's ethanolamine and hydrogen peroxide. The synthesized Nitrogen doped carbon dots and its nano composites were characterized using UV-VIS, FTIR, SEM-EDX, TEM and PL spectroscopic techniques. The UV-Vis peak for N-C-dots is observed at 350 nm and a peak is observed at 268 and 282 nm for Cu/N-Cdot and Ag/N-Cdot composites respectively. This shift in peak towards lower wavelength compared to N-doped C dots due to surface plasma resonance confirms the presence of  $\text{Cu}^{2+}$  and  $\text{Ag}^+$  on the surface of N-doped C

dots. With addition of copper and silver ions to N-CD matrix a blue luminescence is observed instead of Green obtained for pure N-C dots. On comparing the FTIR response between N-Carbon dot, N doped silver and N doped copper carbon dot composites it is clear that the in plane and out of plane bending vibrations of OH at 1300-1500 and at  $650\text{ cm}^{-1}$  and the intensity of C=O vibrational absorption at  $1670\text{ cm}^{-1}$  is decreased in the composites compared to N-Carbon dot confirming that the surface functional groups on carbon dots have been used in the formation of silver and copper carbon dot composite. The elemental composition of synthesized N-CDs and its nanocomposites were identified using EDAX analysis. SEM and HR-TEM studies shows the gives the surface morphologies of prepared samples in nanometer dimensions. It shows that N-Cdot and its composites are spherical in shape. The PL spectra was observed for N-Cdots, Cu/N-Cdots, Ag/N-Cdots. PL response for the synthesised Cu/N-Cdot, Ag/N-Cdot in presence of UA shows a shift towards higher wavelength compared to that of N-CDs and no catalytic effect is observed in presence of metal ions thus functioning as a very good system towards UA sensing. A lowest detection limit towards sensing of UA is found to be 4  $\mu\text{M}$ . The response by the system to sense UA is very fast thus N-Cdot, Cu/N-Cdot, and Ag/N-Cdot function as an effective UA biosensor.

#### Acknowledgement

The authors are grateful to Department of Chemistry, Madras Christian College for their support to carry out this research work.

#### Conflict of interest

All authors declare no conflict of interest.

#### References

- 1 Li P, Sam F & Li Y, Recent advances in fluorescence probes based on carbon dots for sensing and speciation of heavy metals. *Nanophotonics*, 10 (2020) 877.
- 2 Wang H, Gao P, Wang Y, Guo J, Zhang KQ, Du D, Dai X & Zou G, Fluorescently tuned nitrogen-doped carbon dots from carbon source with different content of carboxyl groups. *APL Materials*, 3 (2015)086102.
- 3 Zhang YQ, Ma DK, Zhuang Y, Zhang X, Chen W, Hong LL, Yan QX, Yu K & Huang SM, One-pot synthesis of N-doped carbon dots with tunable luminescence properties. *J Mater Chem*, 22 (2012) 16714
- 4 Jin SH, Kim DH, Jun GH, Hong SH & Jeon S, Tuning the Photoluminescence of graphene quantum dots through the Charge Transfer Effect of Functional Groups. *ACS Nano*, 7 (2012) 1239

- 5 Lim SY, Shen W & Gao Z, Carbon quantum dots and their applications. *Chem Soc Rev*, 44 (2015) 362.
- 6 Kausouni A, Chatzimitakos T & Stalikas C, Bioimaging application of carbon nanodots, *Carbon*, 5 (2019).
- 7 Cao L, Wang X, Meziani MJ, Lu F, Wang H & Luo PG, Carbon dots for multiphoton bioimaging. *J Am Chem Soc*, 129 (2007) 11318.
- 8 Zhao QL, Zhang ZL & Huang BH, Facile preparation of low cytotoxicity fluorescent carbon nanocrystals by electrooxidation of graphite. *Chem Commun*, 44 (2008), 5116.
- 9 Cao L, Meziani MJ, Sahu S & Sun YP, Photoluminescence properties of graphene versus other carbon nanomaterials. *Acc Chem Res*, 46 (2013) 171.
- 10 Li XL, Shi Q, Jin W, Li G, Todoroki K, Mizuno H, Toyo'oka T & Min JZ, Uric acid quantification in fingernail of gout patients and healthy volunteers using HPLC-UV: Quantitative assessment of uric acid in fingernail of gout patients. *Biomed Chromatogr*, 30 (2016) 1338.
- 11 Kaya SI, Kurbanoglu S & Ozkan SA, Nanomaterials-Based Nanosensors for the simultaneous electrochemical determination of biologically important compounds: ascorbic acid, uric acid, and dopamine. *Crit Rev Anal Chem*, 49 (2019) 101.
- 12 Cardoso RM, Silva PRL, Lima AP, Rocha DP, Oliveira TC, do Prado TM, Fava EL, Fatibello-Filho O, Richter EM & Muñoz RAA, 3D-Printed graphene/poly(lactic acid) electrode for bioanalysis: Biosensing of glucose and simultaneous determination of uric acid and nitrite in biological fluids. *Sens Actuators B Chem*, 307 (2020) 127621
- 13 Wang H, Lu Q, Hou Y, Liu Y & Zhang Y, High fluorescence S, N co-doped carbon dots as an ultra-sensitive fluorescent probe for the determination of uric acid. *Talanta*, 155 (2016) 62.
- 14 Xiao N, Liu SG, Mo S, Yang YZ, Han L, Ju YJ, Li NB & Luo HQ, B,N-carbon dots-based ratiometric fluorescent and colorimetric dual-readout sensor for H<sub>2</sub>O<sub>2</sub> and H<sub>2</sub>O<sub>2</sub>-involved metabolites detection using ZnFe<sub>2</sub>O<sub>4</sub> magnetic microspheres as peroxidase mimics. *Sens Actuators B Chem*, 273 (2018) 1735.
- 15 Badoei-dalfard A, Sohrabi N, Karami Z & Sargazi G, Fabrication of an efficient and sensitive colorimetric biosensor based on Uricase/Th-MOF for uric acid sensing in biological samples. *Biosens Bioelectron*, 141 (2019) 111420.
- 16 Shi Y, Pan Y, Zhang H, Zhang Z, Li MJ, Yi C & Yang M, A dual-mode nanosensor based on carbon quantum dots and gold nanoparticles for discriminative detection of glutathione in human plasma. *Biosens Bioelectron*, 56 (2014) 39.
- 17 Chen Y, Lian Y, Huang M, Wei L & Xiao L, A dual-mode fluorometric/colorimetric sensor for Cu<sup>2+</sup> detection based on hybridized carbon dots and gold-silver core-shell nanoparticles. *The Analyst*, 144 (2019) 4250.
- 18 Chen Y, Chang W, Zhu X, Wang R & Tian F, Fluorescence quenching and measurement of captopril in pharmaceuticals, *Indian J Biochem Biophys*, 57 (2020) 270.
- 19 Dong Y, Wang R, Li G, Chen C, Chi Y & Chen G, Polyamine-Functionalized Carbon Quantum dots as Fluorescent probes for selective and sensitive Detection of copper Ions. *Anal Chem*, 84 (2012) 6720.
- 20 Wang Z, Cao L, Ding Y, Shi R, Wang XJ, Lu H, Liu Z, Xiu F, Liu J & Huang W, One step and green synthesis of nitrogen doped carbon quantum dots for multifunctional electronics. *RSC Adv*, 7 (35) (2016) 21969.
- 21 Bharathi D, Krishna RH, Singh V, Kottam N & Siddlingeshwar B, One pot synthesis of C dots and study on its interaction with nano ZnO through fluorescence quenching". *J Lumin*, 5 (2011) 77.
- 22 Zu F & Yan F, The quenching of fluorescence of carbon dots, *Springer*, 184 (2017) 1899.
- 23 Strauss V, Margraf JT, Dolle C, Butz B, Nacken TJ, Walter J, Bauer W, Peukert W, Spiecker E, Clark T & Guldi DM, Carbon nanodots ;towards a comprehensive understanding of their photoluminescence. *J Am Chem Soc*, 136 (2014) 17308.
- 24 Lu Q, Deng J, Hou Y, Wang H, Li H, Zhang Y & Yao S, Hydroxyl-rich C-dots synthesized by a one-pot method and their application in the preparation of noble metal nanoparticles. *Chem Commun*, 51 (2015) 7164.
- 25 Dey D, Bhattacharya T, Majumdar B, Mandani S, Sharma B & Sarma TK, Carbon dot reduced palladium nanoparticles as active catalysts for carbon-carbon bond formation. *Dalton Trans*, 42 (2013) 13821.
- 26 Chen S & Li Y, Inner filter effect based fluorescent sensing systems. *Anal Chim Acta*, 999 (2018) 13.
- 27 Jin JC, Xu ZQ, Dong P, Lai L, Lan JY, Jiang FL & Liu Y, One-step synthesis of silver nanoparticles using carbon dots as reducing and stabilizing agents and their antibacterial mechanisms. *Carbon*, 3 (2015) 1.
- 28 Kargbo O, Jin Y & Ding SN, Recent advances in luminescent carbon dots. *Analytical Chem*, 3 (2016) 1012
- 29 Deng J, Lu Q, Mi N, Li H, Liu M, Xu M, Tan L, Xie Q, Zhang Y & Yao S, Electrochemical synthesis of carbon nanodots directly from alcohols. *Chemistry*, 20 (2014) 4993.
- 30 Paloncy ova MT, Langer M & Otyepka M, Structural Dynamics of Carbon Dots in Water and N,N-Dimethylformamide Probed by All-Atom Molecular Dynamics Simulations. *J Chem Theory Comput*, 14 (2018) 2076.
- 31 Ganiga M & Cyriac J, Understanding the photoluminescence mechanism of nitrogen-doped carbon dots by selective interaction with copper ions. *Chem Phys Chem*, 17 (2016) 2315.
- 32 Dong X, Su Y, Geng H, Li Z, Yang C, Lin X & Zhang. Y, Fast one step synthesis of N doped Carbon dots by pyrolyzingethanolamine. *Mater*, 2 (2012) 7477.
- 33 Yuan.C, Quin X, Xu Y, Shi R, Cheng S & Wang Y Dual-signal uric acid sensing based on carbon quantum dots and o-phenylenediamine *Spectrochim Acta Part A: Mol Biomol Spectrosc*, 254 (2021) 119678.
- 34 Zu F, Yan F, Bai Z, Xu J, Wang Y, Huang Y & Zhou X, Surface modification and chemical functionalization of carbon dots: a review. *Microchimica Acta*.184 (2017) 1899.
- 35 Wang X, Cao L, Lu F, Meziani M J, Li H, Qi G, Zhou B, Harruff BA, Kermarec F & Sun YP, Photoinduced electron transfers with carbon dots. *Chem Commun*, 25 (2009) 3774
- 36 Ren X,W,Wang P, Bunker CE, Colema M, Teisl R, Cao L & Sun YP, A New Approach in functionalization of carbon nanoparticles for optoelectronically relevant carbon dots and beyond. *Carbon*, 141 (2019) 553.

- 37 Wang Li, Cao HX, Pan CG, He YS, Liu HF, Zhou LH & Li CQ, Liang GX, Recent progress in copper nanocluster-based fluorescent probing: a review. *Microchimica Acta*. 186 (2019) 28.
- 38 Ding H, Bo S, Wei YS & Xiong HM, Full-Color light-emitting carbon dots with a surface-state-controlled luminescence mechanism. *ACS Nano* 10(2016)484.
- 39 Barman S & Sadhukhan M, Facile bulk production of highly blue fluorescent graphitic carbon nitride quantum dots and their application as highly selective and sensitive sensors for the detection of mercuric and iodide ions in aqueous media *J Mater Chem*, 41 (2012) 21832.
- 40 Song Y, Zhu C, Song J, He Li H, Du D & Lin Y, Drug-Derived bright and color-tunable n-doped carbon dots for cell imaging and sensitive detection of  $Fe^{3+}$  in living cells. *ACS Appl. Mater. Interfaces*, 9 (2017) 7399.
- 41 Dimos K, Carbon quantum dots: Surface passivation and functionalization. *Curr Org Chem*, 20 (2018) 682.
- 42 Nguyen V, Si J, Yan L & Hou X, Electron-hole recombination dynamics in carbon nanodots. *Carbon*, 95 (2015) 659.
- 43 Shen L, Chen M, Hu L, Chen X & Wang J, Growth and stabilization of silver nanoparticles on carbon dots and sensing application. *Langmuir*, 29 (2013) 16135.
- 44 Hallaj T, Azizi N & Amjadi M, A dual-mode colorimetric and fluorometric nanosensor for detection of uric acid based on N, P co-doped carbon dots and in-situ formation of Au/Ag core-shell nanoparticles. *Microchemical J*, 162 (2021) 105865.